Investigation into the Interactions between Diadenosine 5′,5‴-P^1,P^4-Tetraphosphate and Two Proteins: Molecular Chaperone GroEL and cAMP Receptor Protein†

Julian A. Tanner, Michael Wright, E. Margaret Christie, Monika K. Preuss, and Andrew D. Miller*

Imperial College Genetic Therapies Centre, Department of Chemistry, Flowers Building, Armstrong Road, Imperial College London, London SW7 2AZ, U.K.

Received December 12, 2005; Revised Manuscript Received January 13, 2006

ABSTRACT: Diadenosine 5′,5‴-P^1,P^4-tetraphosphate (Ap_4A) is a dinucleoside polyphosphate found ubiquitously in eukaryotic and prokaryotic cells. Despite Ap_4A being universal, its functions have proved to be difficult to define, although they appear to have a strong presence during cellular stress. Here we report on our investigations into the nature and properties of putative Ap_4A interactions with *Escherichia coli* molecular chaperone GroEL and cAMP receptor protein (CRP). We confirm previous literature observations that GroEL is an Ap_4A binding protein and go on to prove that binding of Ap_4A to GroEL involves a set of binding sites (one per monomer) distinct from the well-known GroEL ATP/ADP sites. Binding of Ap_4A to GroEL appears to enhance ATPase rates at higher temperatures, encourages the release of bound ADP, and may promote substrate protein release through differential destabilization of the substrate protein−GroEL complex. We suggest that such effects should result in enhanced GroEL/GroES chaperoning activities that could be a primary reason for the improved yields of the refolded substrate protein observed during GroEL/GroES-assisted folding and refolding at ≥30 °C in the presence of Ap_4A. In contrast, we were unable to obtain any data to support a direct role for Ap_4A interactions with CRP.

Members of the unusual dinucleoside polyphosphate class of compounds are present in an enormous variety of cell types. While the family's intra- and intercellular functions remain ambiguous (see reviews *1*−*3*), both Ap_4A[1] and its apparently antagonistic cousin Ap_3A (*4*−*6*) have been strongly linked to the prokaryotic heat shock response and may be considered modulators (and perhaps "alarmones") of cellular stress (*7*, *8*) in both prokaryotes and eukaryotes. In 1991, Johnstone and Farr (*9*) used a radio/affinity-labeled Ap_4A analogue ([^{32}P]-8-azido-Ap_4A) and a SDS−PAGE autoradiography procedure to identify at least 12 *Escherichia coli* Ap_4A-binding proteins from lysate. These included stress proteins GroEL (Cpn60), DnaK (Hsp70), and ClpB (Hsp100). Of these, the most familiar is probably GroEL, a homologue of the eukaryotic hsp60 family of molecular chaperone/stress proteins.

GroEL is a large homo-oligomeric protein comprised of 14 identical monomeric polypeptides (57 kDa each) arranged in two stacked rings of seven monomers. Each ring encloses a central cavity where unfolded protein substrate molecules may be sequestered for protection against aggregation. GroEL is normally associated with a co-molecular chaperone protein known as GroES, a smaller homo-oligomeric protein comprised of seven identical monomeric polypeptides (10 kDa each) arranged in a single ring. Both GroEL and GroES have been extensively studied (*10*−*13*), and the mechanism of the GroEL/GroES molecular chaperone machine (powered by ATP → ADP hydrolysis) is now quite well understood (*14*−*21*). The identification of GroEL as an *E. coli* Ap_4A-binding protein by Johnstone and Farr was accompanied by two other significant observations. First, overproduction of GroEL by epichromosomal plasmid expression was found to result in enhanced [^{32}P]Ap_4A labeling of intracellular GroEL. Second, unlabeled ATP was found not to compete with labeled Ap_4A for binding to GroEL, suggesting that GroEL might have distinct and separate binding sites for ATP and Ap_4A, respectively (*9*). In other mechanistic studies, Farr et al. showed that while *apaH*$^-$ (an Ap_4A hydrolase) strains of *E. coli* were significantly less heat resistant, this defect was partially rescued by the introduction of plasmid DNA encoding ClpB (*22*). This suggested that ClpB−Ap_4A interactions were acting to moderate the normally fatal effects of high levels of Ap_4A, effectively rendering cells much less thermo-sensitive.

Farr et al. also observed that increased levels of Ap_4A (up to 100 μM) rendered bacteria nonmotile and unable to biosynthesize the enzymes required for lactose and galactose

† E.M.C. thanks the EPSRC for a studentship. We thank Mitsubishi Chemical Corp. and IC-Vec Ltd. for supporting the Imperial College Genetic Therapies Centre.

* To whom correspondence should be addressed. Telephone: +44 207 594 5773. Fax: +44 207 594 5803. E-mail: a.miller@imperial.ac.uk.

[1] Abbreviations: αLA, α-lactalbumin; AMPPCP, adenosine 5′-(β,γ-methylene)triphosphate; Ap_3A, diadenosine-5′,5‴-P^1,P^3-triphosphate; Ap_4A, diadenosine 5′,5‴-P^1,P^4-tetraphosphate; cAMP, adenosine 3′,5′-cyclic monophosphate; CD, circular dichroism; ClpB, 100 kDa heat shock protein; CRP, cAMP receptor protein; dial, dialdehyde affinity labeling group; DnaK, 70 kDa heat shock protein; DSC, differential scanning calorimetry; dsDNA, double-stranded DNA; DTT, dithiothreitol; FPLC, fast protein liquid chromatography; GroEL, 60 kDa chaperonin; GroES, 10 kDa chaperonin; GuHCl, guanidinium hydrochloride; HEPES, 4-(2-hydroxyethyl)-1-piperazineethanesulfonic acid; IAEDANS, *N*-iodoacetyl-*N*′-(5-sulfo-1-naphthyl)ethylenediamine fluorophore; ITC, isothermal titration calorimetry; L-LDH, L-lactic dehydrogenase; LysU, lysyl-tRNA synthase (heat inducible isozyme); mant, *N*-methylanthraniloyl fluorophore; mMDH, mitochondrial malate dehydrogenase; MMCO, molecular mass cutoff; NADH, nicotinamide adenine dinucleotide; PMI, parent molecular ion; PMSF, phenylmethanesulfonyl fluoride; Tris-HCl, buffered tris(hydroxymethyl)-aminomethane.

10.1021/bi052529k CCC: $33.50
Published on Web 02/11/2006

metabolism (*22*). In *E. coli*, the cyclic AMP receptor protein (CRP, also known as catabolite gene activator protein, CAP) is primarily responsible for the control of such metabolism. CRP is homodimeric protein (47 kDa) possessing two pairs of cAMP binding sites, one high-affinity site and one low-affinity site per monomer (*1*−*3*, *23*−*26*). CRP binds cAMP when available (physiological [cAMP] < 1 μM) (*27*) to form a CRP−$cAMP_1$ complex with two molecules of cAMP bound in the two higher-affinity sites. The CRP−$cAMP_1$ complex recognizes and binds to specific *E. coli* DNA loci that closely match a 22 bp consensus sequence (AAATGTGATCTAGATCACATTT) in the promoter region of the *lac* operon among others (*28*−*32*). The combined CRP−$cAMP_1$−DNA complex then simulates operon transcription by RNA polymerase and subsequent translation of enzymes and other operon proteins. The CRP−$cAMP_1$ complex is a positive regulator at more than 100 promoter sites, including those related to the catabolism of secondary sugars and those involved in the regulation of cellular processes such as cell motility (*33*−*36*). There have been a number of reports describing how Ap_4A has a direct negative effect on the transcriptional activation of all operons under the control of the CRP−$cAMP_1$ complex (*22*, *24*, *25*), suggesting that Ap_4A is able to disrupt the function of the CRP−$cAMP_1$ complex. Therefore, either CRP or the CRP−$cAMP_1$ complex has been considered as a potential intracellular target of Ap_4A.

Given the foregoing evidence, we undertook a series of experiments designed to improve our understanding of the interactions between GroEL and Ap_4A on one hand and potential interactions between CRP or the CRP−$cAMP_1$ complex and Ap_4A on the other. Here we report the results of binding studies between Ap_4A and GroEL followed by functional characterization assays. We also report upon our attempts to characterize interactions involving CRP and Ap_4A. The GroEL−Ap_4A interactions appear to be more obviously meaningful and suggest at least one clear intracellular role for Ap_4A in managing the stress responses in *E. coli*.

MATERIALS AND METHODS

Materials. All chemicals and reagents were obtained from Sigma-Aldrich or VWR International unless otherwise stated. EZ-LinkTM sulfosuccinimidyl-6′-(biotinamido)-6-hexanamido hexanoate (sulfo-NHS-LC-LC-biotin), ImmunoPureTM Avidin, 2-hydroxyazobenzene-4′-carboxylic acid (HABA), and streptavidin were obtained from Pierce. Ten-base pair (bp) DNA molecular weight markers and E-gels were from Invitrogen. Chromatography steps were carried out using columns connected to an Amersham Biosciences FPLC system monitoring elution by absorption at 254 nm. Nucleotide and polyphosphate purities were checked on a SOURCE 15Q anion exchange column (Amersham Biosciences) using a 0−0.5 M NaCl gradient. ATP, cAMP, and Ap_4A were all estimated from peak integration to be >95% pure. Concentrations were measured using the following extinction coefficients: $\epsilon_{259} = 15\,400\ M^{-1}\ cm^{-1}$ for ATP, $\epsilon_{258} = 14\,650\ M^{-1}\ cm^{-1}$ for cAMP, and $\epsilon_{260} = 27\,100\ M^{-1}\ cm^{-1}$ for Ap_4A (*26*, *37*); $\epsilon_{278} = 40\,800\ M^{-1}\ cm^{-1}$ for CRP (*28*); $\epsilon_{260} = 50\ \mu g^{-1}\ mL^{-1}\ cm^{-1}$ for for dsDNA (*29*); $\epsilon_{278} = 61\,160\ M^{-1}\ cm^{-1}$ for LysU [calculated from amino acid sequence by the method of Gill and von Hippel (*38*)]; $A_{280}^{1\%} = 11.3$ for L-LDH (quoted by Sigma Aldrich); and $A_{280}^{1\%} = 2.5$ for mMDH (*39*). Protein concentrations are given as their oligomer concentrations unless stated otherwise, and they were considered to be effectively nucleotide free if A_{280}/A_{260} was greater than 1.5 (*29*). Experiments were carried out at room temperature unless otherwise indicated, and Milli-Q water (Millipore, Billerica, MA) was used throughout.

Expression and Purification of GroEL and GroES. All experiments involving the GroE system were carried out with the chaperone protein purified from *E. coli* strain TG2. This was transformed with plasmid pAM1, providing a recombinant strain, TG2/pAM1, that is able to overexpress both GroEL and GroES. The construction of pAM1, its transformation into *E. coli* TG2 cells, and the growth of TG2/pAM1 are described by Hutchinson et al. (*40*). *E. coli* cells were grown in 20 L cultures and provided as a homogenized frozen cell paste. GroEL and GroES were purified free of aromatic impurities from *E. coli* TG2/pAM1 cell paste according to procedures outlined by Tabona et al. (*41*) and Preuss et al. (*42*). The concentrated, purified solutions of both GroEL and GroES were dialyzed into 50 mM Tris-HCl (pH 7.6) containing 2 mM DTT at 4 °C. Then glycerol was added to a final concentration of 50% (v/v) so that samples could be stored at −20 °C without freezing. The activity of the chaperone proteins stored under these conditions was found to be undiminished over many months (*42*). Concentrations of GroEL or GroES were determined by $A_{280}^{1\%}$ values calibrated by quantitative amino acid analysis for each sample and expressed in terms of monomer or oligomer concentrations as appropriate (*41*).

Expression and Purification of CRP. E. coli strain PP47-pHA7 carrying the crp gene (*48*) was grown in YT/ampicillin medium. After the cells were harvested, the CRP was purified using a process based on that of Ryu et al. (*30*) with several crucial modifications. Cells were suspended in an initial lysis buffer comprised of 50 mM Tris-HCl (pH 8.0) with 50 mM KCl, 10% (w/v) sucrose, 1 mM DTT, 0.1 mM EDTA, 0.4 mg/mL lysozyme, and 1 mM protease inhibitors (PMSF, pepstatin, and aprotinin), before sonication and DNA precipitation. After centrifugation, the protein supernatant was fractionated with ammonium sulfate and the 30−60% pellet dissolved in 50 mM HEPES (pH 7.6) containing 50 mM KCl and 0.5 mM DTT (4 mL) and then loaded onto a MonoS cation exchange column (Amersham Biosciences) in the same buffer. The protein was eluted with a linear gradient (40 mL) from 50 to 400 mM KCl at a flow rate of 1 mL/min. Subsequent analysis of combined fractions by SDS−PAGE showed CRP to be >95% pure (Coomassie blue staining). CRP was stored in 50 mM potassium phosphate (pH 7.0) containing 0.5 M KCl, 0.2 mM DTT, 0.2 mM EDTA, and 50% (v/v) glycerol at 4 °C. A typical purification yielded approximately 20 mg/L.

Synthesis and Hybridization of Oligonucleotides. Custom-made oligonucleotides were synthesized by Transgenomic (Omaha, NE) using the phosphoramidite method and purified by HPLC. The sequences of the sense and antisense strands of the 40 bp consensus and control DNA molecules are shown (Scheme 1). For interaction analysis (IAsys) experiments, the sense strands were each labeled with biotin at the 5′ termini in both cases (see Scheme 1). Each individual sense and complementary oligonucleotide was suspended in 10 mM Tris-HCl (pH 7.8) containing 50 mM NaCl and 1 mM EDTA. Equimolar amounts of corresponding sense and

Scheme 1: Sense and Antisense Strands for Consensus and Control DNA

consensus DNA

```
5'-GCAACGCAATAAATGTGATCTAGATCACATTTTAGGCACCC-3'
 3'-GTTGCGTTATTTACACTAGATCTAGTGTAAAATCCGTGGGG-5'
```

control DNA

```
5′-GTACCATACGATATCAAGTTAGCCCGGTATGTTCAAAACAC-3'
 3'-ATGGTATGCTATAGTTCAATCGGGCCATACAAGTTTTGTGG-5'
```

complementary oligonucleotides were then combined and heated to 90 °C prior to being cooled to 25 °C at a rate of 1 °C/min, thereby producing a good yield of duplex DNA. The resulting consensus DNA and control DNA duplexes were then extensively dialyzed into 50 mM Tris-HCl (pH 7.8) containing 100 mM KCl and 1 mM EDTA, Individual aliquots were then stored at −25 °C.

Synthesis of Dial-mant-Ap_4A. The synthesis of dial-mant-Ap_4A (Figure 1) via a tandem synthetic−biosynthetic procedure has been previously described (*43*, *44*) and will only be specifically summarized here. Purified mant-Ap_4A (100 mg, 0.101 mmol) was dissolved in deionized water (3 mL), before being carefully oxidized by 0.3 M aqueous $NaIO_4$ (∼80 μL), added in aliquots (5−10 μL) with vortex stirring following each addition. The reaction was monitored using an HPLC system equipped with a SOURCE 15Q (Amersham Biosciences) anion exchange column, in which reaction mixture aliquots were loaded in 20 mM Tris-HCl (pH 8.0) and eluted with a 0 to 0.6 M gradient of NaCl at 2 mL/mL over 16 mL. Nucleotides and polyphosphates were detected by an increase in absorbance at 260 nm against a background at 310 nm. Oxidation caused a slight increase in the mant-Ap_4A retention time and was judged to be complete when no further increase was seen upon addition of further $NaIO_4$. The solution was then diluted with ethanol to 50% (v/v) before freeze-drying. The resulting light tan powder was extracted with 98% ice-cold ethanol in three 1 mL portions, which were combined and stored at −20 °C. Electrospray ionization mass spectroscopy showed a $[M - H]^-$ of *m*/*z* 965.6 and 983.8 (100%, −ve setting) which matches dial-mant-Ap_4A and its sodium salt. Ion exchange HPLC showed the analogues to have a purity of >90% with respect to other nucleotides and polyphosphates. The extinction coefficient of the fluorescently labeled affinity probe was estimated to be 28 500 M^{-1} cm^{-1} (ϵ_{260}).

Circular Dichroism. Spectra were recorded on a J-715 spectropolarimeter (Jasco, Easton, MD) in a 1 cm path-length cuvette between 320 and 220 nm, using a 5 nm bandwidth, a 10 mdeg sensitivity, 4 s response times, and a scan rate of 10 nm/min. For the CD titration binding assays, the cuvette contained a stirred solution of Ap_4A (20 μM) in 20 mM Tris-HCl (pH 8.0, 1.5 mL) maintained at 20 °C, in the presence or absence of 10 mM $MgCl_2$, 10 mM KCl, 10 mM EDTA, or 0.5 mM ADP as required. Reactive Red-purified GroEL (*42*) was concentrated in 30 kDa MMCO centricons after dialysis to reduce the volumetric changes during the titration to below 1%. Ap_4A exhibits a substantial negative maximum signal at ΔA_{279} that disappears as GroEL is added. After each titration binding experiment, data were background corrected and $\Delta\Delta A_{279}$ data plotted as a function of GroEL concentration.

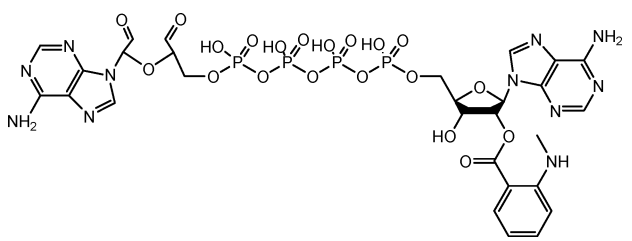

FIGURE 1: Structure of fluorescently labeled Ap_4A analogue affinity probe, dial-mant-Ap_4A.

Isothermal Calorimetry (ITC). Measurements were carried out with a VP-ITC calorimeter (Microcal, Northampton, MA) interfaced with a computer. Solutions containing ADP or GroEL were all prepared in 25 mM Tris-HCl (pH 8.0) containing 10 mM $MgCl_2$ and 10 mM KCl. These were then centrifuged (13000*g* for 5 min) before being used and subjected to vacuum degassing for 5 min with gentle stirring. Afterward, the solution of ADP (750 μM) was taken up in an injection syringe (250 μL) and slowly titrated into the ITC sample cell which contained a solution of GroEL (2.5 μM, monomer concentration) either with or without added Ap_4A (100 μM). The reference cell, which acts only as a thermal reference to the sample cell, was filled with water. Titrations typically consisted of a preliminary 1 μL injection followed by 25 × 10 μL injections with a duration of 20 s each, with 3 min spacing between. Alternatively, a regime of 50 × 5 μL injections with a duration of 10 s was used. All experiments were performed at 20 °C. Data from the first injection were discarded as being unreliable due to diffusion between the syringe and cell solutions. The remaining data were corrected for the heat of dilution of ADP into the Tris-HCl buffer and then used to obtain binding isotherms that were fitted to the Origin models by Marquardt nonlinear least-squares analysis (Origin version 5.0, Microcal).

Differential Scanning Calorimetry (DSC). Studies were performed using a VP-DSC differential scanning calorimeter (Microcal, Northampton, MA) employing a scan rate of 60 °C/h. Prior to the experiment, all solutions of GroEL were extensively dialyzed against 25 mM Tris-HCl (pH 8.0), before the addition of various other components as appropriate, including Ap_4A, $MgCl_2$, and unfolded α-lactalbumin (αLA). The αLA was unfolded before being used in 25 mM Tris-HCl (pH 8.0) containing 1 mM DTT and 1 mM EDTA according to literature (*45*). After the combination of appropriate components with GroEL in solution, resulting mixtures were then subjected to further vacuum degassing for 10 min prior to experimentation. The reference cell was filled with the external buffer from dialysis. Thereafter, scans were carried out and repeated twice to confirm the irreversibility of the denaturing thermal transitions. Buffer−buffer controls were also run, and data analysis carried out following buffer−buffer baseline subtraction. Calorimetric data were then analyzed using Origin version 5.0 provided by MicroCal Inc.

ATPase Hydrolysis Assays. Studies were carried out on a computer-attached 1100 HPLC system (Agilent, Palo Alto,

CA) equipped with a 2 mL SOURCE Q ion exchange column (Amersham Biosciences) and a thermostat-controlled injection chamber. The column was loaded and washed with 10 mM Tris-HCl (pH 8.0), and fractions were eluted with a gradient from 0 to 300 mM NaCl. Mixtures of GroEL (0.5 μM, homo-oligomer concentration) in 10 mM Tris-HCl (pH 8.0) containing 10 mM $MgCl_2$, 10 mM KCl, and Ap_4A (up to 100 μM) were made up in batches (each 500 μL). ATP (3 mM) was added, and then individual batches were transferred to the HPLC injection chamber. Batches were incubated at a variety of temperatures (25, 31, and 37 °C), and injection aliquots were then taken automatically every 8 min. Nucleotides and polyphosphates were detected by an A_{259} absorbance sensor and were identified by their retention time in comparison to known standards. Relative concentrations were calculated from peak areas. ATP and ADP stocks were confirmed to be 98% pure before they were used; the Ap_4A stocks contained some ADP and AMP and were estimated to be 95% pure. Similar assays were carried out by incubating GroEL with either AMP (3 mM), ADP (3 mM), or Ap_4A (3 mM) in place of ATP, but no hydrolysis was seen in any case except for ATP.

Gel Retardation. This method was based on that of Garner and Revzin (*46*) and Fried and Crothers (*47*). Samples containing combinations of CRP with cAMP were analyzed for their DNA binding behavior in the presence and absence of Ap_4A (182 μM). Binding mixtures (20 μL each) were prepared by the consecutive addition of water, CRP, nucleotide, and/or Ap_4A and DNA to give the correct final concentrations. After a 20 min incubation at 25 °C, loading buffer (4 μL) was added and the combined mixtures were applied to a 4% E-gel. Gels were resolved by electrophoresis, and DNA bands were visualized finally by using added ethidium bromide.

Resonant Mirror Interaction Assay (IAsys). Changes in the refractive index occurring due to biological interactions were studied using a ThermoLabsystems Affinity Sensors IAsys+ resonant mirror biosensor, in conjunction with a two-well biotin cuvette (one used as a control). The cuvette was activated with streptavidin, and then either consensus or control DNA was immobilized onto the surface according to previously established protocols (*48*). Regeneration was performed using 3 M $MgCl_2$ (40 μL) for 2 min followed by 20 mM potassium phosphate (pH 6.5) (3 × 50 μL) until there was no further change in instrument response. The cuvette was then equilibrated in 50 mM potassium phosphate (pH 7.8) with 100 mM KCl, 1 mM EDTA, and 0.05% Tween 20 until a stable baseline was obtained. Thereafter, this same buffer was used throughout for all binding experiments. The concentration of immobilized consensus or control DNA was estimated from the instrument response to be 10−100 μM.

CRP, cAMP, Ap_4A, and ATP were premixed in small volumes (2−10 μL), giving the indicated final concentrations, prior to administration to the cuvette. Association was then monitored (5−10 min), after which dissociation was provoked by administration of 50 mM potassium phosphate (pH 7.8) with 100 mM KCl, 1 mM EDTA, and 0.05% Tween 20 (3 × 50 μL). Dissociation was also monitored (5−10 min) prior to regeneration of the cuvette in preparation for the next experiment. Instrument responses (Y_t) corresponding to both association and dissociation data were fitted using eqs 1 and 2, respectively. The full derivation of these equations can be found in George et al. (*49*).

$$Y_t = (Y_\infty - Y_o)[1 - \exp(-k_{on}t)] + Y_o \quad (1)$$

$$Y_t = Y_o[\exp(-k_{diss}t)] \quad (2)$$

where Y_o, Y_t, and Y_∞ represent the response at the initial time, time t, and final equilibrium, respectively, k_{on} is the observed rate constant (eq 3) for an experiment carried out at a particular ligand concentration [L], while k_{ass} and k_{diss} represent the rate constants for association and dissociation processes, respectively. Equilibrium response values were calculated as a direct measure of the amount of complex formed at equilibrium as a function of [L].

$$k_{on} = k_{diss}[L] + k_{diss} \quad (3)$$

Mitochondrial Malate Dehydrogenase Refolding Assay. mMDH (0.3 mg/mL) was unfolded by dissolution in a denaturing buffer [50 mM potassium phosphate (pH 7.6) with 20 mM DTT, 10 mM EDTA, and 3 M GuHCl]. This denaturing solution was incubated for 2 h to fully unfold mMDH. Thereafter, refolding was initiated by diluting unfolded mMDH (final concentration of 10 μg/mL; 143 nM) into refolding buffer [150 mM sodium phosphate (pH 7.6) containing 2 mM DTT, 10 mM $MgCl_2$, 10 mM KCl, and 2 mM ATP] with GroEL (860 nM, oligomer concentration) and GroES (1720 nM, oligomer concentration) present for molecular chaperone-assisted folding. Solutions were then incubated at 20 °C for 2−3 h, and the extent of mMDH refolding was monitored with time by removing aliquots of the refolding mixture at set time intervals and measuring the level of mMDH enzyme activity in each of these aliquots in turn. Typically, each aliquot (20 μL) was combined immediately postremoval with an assay buffer of 150 mM sodium phosphate (pH 7.6) with 2 mM DTT, 0.5 mM oxaloacetate, and 0.2 mM NADH (980 μL) preincubated at 30 °C. The initial rate of conversion of NADH to NAD^+ was then determined ($-dA_{360}/dt$), and the result was expressed as a percentage of the initial rate of conversion of NADH to NAD^+ measured using a normalized sample of native mMDH kept under the same conditions of concentration, ionic strength, buffer, and pH as refolding mMDH. The effect of GroEL/GroES on mMDH refolding was examined at a sequential variety of temperatures, namely, 30, 37, and 42 °C, in the presence and absence of Ap_4A (200 μM).

Affinity Probe Labeling of Proteins. The ability of GroEL to specifically bind Ap_4A was investigated with a novel procedure using dial-mant-Ap_4A as an affinity binding site probe (Figure 1). Solutions of GroEL, *E. coli* lysyl-tRNA synthase (LysU, positive control), and rabbit muscle L-lactic dehydrogenase (L-LDH, negative control) were prepared in 20 mM HEPES (pH 8.0) with 10 mM $MgCl_2$ and 10 mM KCl. An aliquot (100 μL) of each protein solution (50 μM final oligomer concentration) in turn was then combined with an aliquot (100 μL) of a dial-mant-Ap_4A solution (final concentration of 50 μM) in the same buffer, giving a labeling mixture which was then subjected to initial vortex mixing. After 1 h at room temperature, each labeling mixture was then vortex mixed again and applied individually to separate 4 mL, 10 kDa molecular mass cutoff centricons for concen-

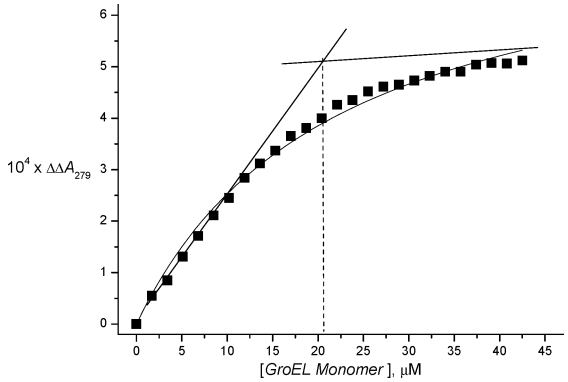

FIGURE 2: Titration observed by circular dichroism of Ap_4A (20 μM) in 20 mM Tris-HCl at pH 8.0 and 20 °C, with GroEL (at the indicated monomer concentrations). Negative CD maximum ΔA_{279} results from adenine base stacking and is disrupted when the polyphosphate binds to GroEL. The stoichiometry of Ap_4A binding was determined as one Ap_4A per GroEL monomer by Klotz tangents.

tration by centrifugation (4000*g*) to a minimal volume. After repeated dilution with buffer (3 mL) and subsequent dilution (back to approximately 100 μL), the residue was then analyzed for mant fluorescence. Fluorescence emission spectra (400−500 nm) were measured with a RF-5301PC spectrofluorophotometer (Shimadzu, Kyoto, Japan) using an excitation wavelength of 356 nm and high sensitivity. To give the best signal-to-noise ratio within the machine's range, the excitation monochromator slits were set to 3 nm and the emission slit was set to 5 nm. The sampling interval was 1 nm, and data were collected by a computer before analysis. Blank spectra of all proteins in probe free buffer were also measured and were subtracted from the results before analysis. Reported results are the mean average of three scans, and each labeling procedure was repeated in triplicate to confirm the results.

RESULTS

Studies with GroEL. Interactions of Ap_4A with GroEL (*41*, *42*) were studied initially by circular dichroism (CD) spectroscopy. In free solution, Ap_4A exhibits a distinct reverse Cotton effect between 240 and 300 nm with a negative maximum ΔA_{279} that derives from intramolecular base stacking (*50*). If the binding of Ap_4A to a bona fide Ap_4A binding protein requires base destacking, then the determination of equilibrium binding constants should be made possible by monitoring changes in ΔA_{279} ($\Delta\Delta A_{279}$) as a function of concentration. In this case, a reverse CD titration binding experiment was performed in which a fixed concentration of Ap_4A was titrated with increasing amounts of GroEL until saturation, and then $\Delta\Delta A_{279}$ data were plotted as a function of GroEL concentration and fitted to give the illustrated saturation binding isotherm (Figure 2). From these data, an apparent dissociation constant ($K_{d,app}$) of 10 ± 2 μM was determined. Furthermore, by using Klotz tangents (*51*), the binding stoichiometry was found to be one Ap_4A per monomer of GroEL (Figure 2). With the assumption that binding sites are independent and are of equal affinity, actual site dissociation constants (κ_d) may be estimated with eq 4:

$$\kappa_d = nK_{d,app} \quad (4)$$

where n is the total number of binding sites. Hence, given the observed stoichiometry, n must be 14, and hence, κ_d becomes 140 ± 30 μM. The binding of Ap_4A to GroEL was able to take place in the presence of 10 mM EDTA, suggesting that metal cations were not required, although the presence of 10 mM Mg^{2+} and/or K^+ did not interfere. In contrast, the addition of Zn^{2+} [for which Ap_4A has been previously reported to have a high affinity (*52*)] appeared to disrupt the intramolecular base stacking, substantially reducing the Cotton signal and masking any changes upon titration with GroEL. GroEL−Ap_4A binding was unaffected by ADP concentrations up to 0.5 mM (in 10 mM $MgCl_2$ and 10 mM KCl) prior to induced protein aggregation (data not shown), thereby suggesting that Ap_4A was binding to sites on GroEL distinct from the well-known ATP/ADP binding sites located in the central domain of each GroEL monomer.

Further proof of a new dinucleotide binding site on each GroEL monomer was obtained using the novel fluorescently labeled Ap_4A analogue affinity probe (dial-mant-Ap_4A, Figure 1) that was designed and synthesized by extrapolation from our previous work with fluorescent polyphosphate analogues (*43*). Dial-mant-Ap_4A is equipped with an *N*-methylanthraniloyl (mant) fluorophore that exhibits intense fluorescence in water [I_{max} = 448 nm (light blue); A_{max} = 356 nm], with an I_{max} which becomes characteristically blue-shifted with a concurrent increase in fluorescence quantum yield (4−5-fold in 50% ethanol) upon contact with a more hydrophobic binding environment (*53*). Dial-mant-Ap_4A is also equipped with a dialdehyde (dial) that is capable of forming covalent Schiff bases with amine functional groups within, or in the vicinity of, the Ap_4A binding sites of bona fide Ap_4A binding proteins (*44*, *54*).

Dial-mant-Ap_4A affinity probe binding assays were performed using GroEL, LysU (positive control, known Ap_4A binding protein), and L-LDH (negative control, not an Ap_4A binding protein). In each case, dial-mant-Ap_4A was combined and incubated with the protein prior to removal of excess unbound affinity probe by means of a 10 kDa molecular mass cutoff centrifugal concentrator. As expected, at the conclusion of the affinity probe experiment, LysU was extensively fluorescently labeled and L-LDH was not (Figure 3). Consistent with the CD evidence that GroEL is an Ap_4A binding protein, GroEL was also found to be extensively fluorescently labeled to an extent equivalent to that of LysU. However, in the presence of ADP or ATP, dial-mant-Ap_4A was largely prevented from labeling LysU presumably due to binding site competition. LysU is homodimeric with two well-defined catalytic active sites able to bind ATP or ADP. Dial-mant-Ap_4A and by implication Ap_4A must therefore bind to LysU at the same binding sites. By contrast, dial-mant-Ap_4A was still capable of extensive fluorescent labeling of GroEL even in the presence of ADP or β,γ-methylene-ATP (AMPPCP), thereby suggesting that dial-mant-Ap_4A and by implication Ap_4A must bind to GroEL at binding sites that are distinct and different from the well-known GroEL ADP/ATP binding sites.

Given the fact that both CD titration binding experiments and affinity probe binding studies appeared to support previous observations (*9*) and interlock to support the existence of a distinct Ap_4A binding site per GroEL monomer, separate from the ATP/ADP binding site, we elected to devise experiments in an attempt to understand

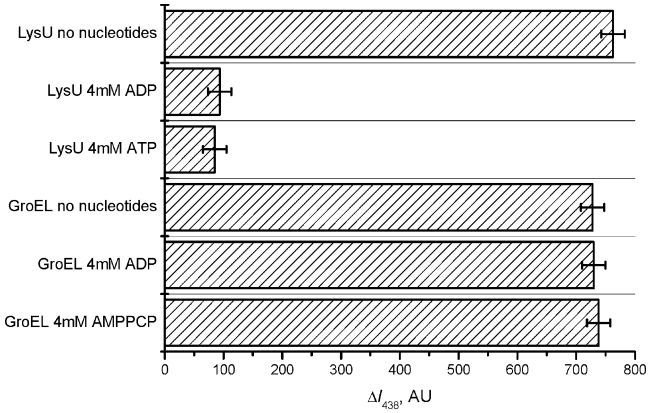

FIGURE 3: Fluorescently labeled affinity probe labeling of proteins by dial-mant-Ap_4A. GroEL, LysU, and L-LDH (all at 50 μM, oligomer concentrations) are incubated separately with dial-mant-Ap_4A (50 μM) for 1 h, and the extent of affinity labeling is determined by observing protein fluorescence spectra (excitation at 356 nm) post-"washing". Experiments were repeated in the presence of ADP (4 mM), ATP (4 mM), or nonhydrolyzable ATP analogue β,γ-methylene-ATP (AMPPCP) (4 mM) to demonstrate binding competition.

the potential role of binding of Ap_4A to GroEL. Previously, interactions between nucleotides and GroEL have been studied by a number of techniques, including isothermal titration calorimetry (ITC). ITC measures the heating or cooling required to maintain a solution of a "receptor" at constant temperature, during titration with aliquots of solution in which a "ligand" is dispersed. After correction for heats of dilution, the enthalpy of binding is determined directly by data curve fitting, from which values of equilibrium binding constants may be derived. Binding of Ap_4A to GroEL was observed to be enthalpically neutral and therefore difficult to observe by ITC. By contrast, binding of ADP to GroEL was clearly observable, as described by others previously (*55*). In our hands, ADP (0−750 μM) interacting with GroEL (2.5 μM monomer concentration) in the presence of Mg^{2+} and K^+ ions (10 mM each) was moderately exothermic, and after analysis, the dissociation constant for the interaction (K_d) was calculated to be 37 ± 24 μM with an expected stoichiometry of one ADP binding per GroEL monomer. When this titration was repeated in the presence of 100 μM Ap_4A, the value of K_d was reduced to 101 ± 45 μM, leaving the binding stoichiometry unchanged (Figure 4). While plot errors are large, ADP does appear to undergo a 3-fold decrease in binding affinity as a result of the presence of Ap_4A at high physiological concentrations. Clearly, the character of binding of Ap_4A to GroEL and the character of binding of ADP to GroEL are different. Exothermic binding events are frequently associated with significant salt-link and H-bond formation. Mildly endothermic binding events are frequently associated with binding through the hydrophobic effect, where binding is driven largely by entropic considerations and involves only the weaker noncovalent interactions. Therefore, binding of ADP to GroEL fits the first category, and binding of Ap_4A to GroEL appears to involve a mixed-mode form of binding interaction. The consequences of binding of Ap_4A do appear to involve a 3-fold reduction in ADP binding affinity, suggesting that Ap_4A binding exercises a mild negative cooperativity on ADP binding.

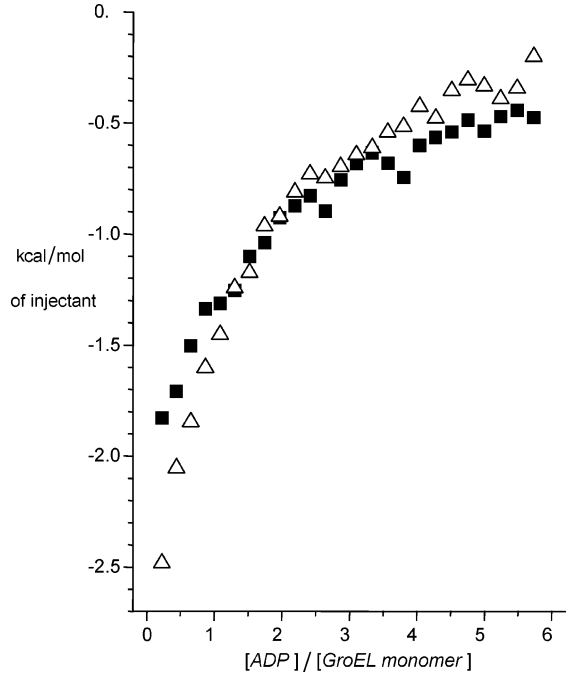

FIGURE 4: Titration of GroEL (2.5 μM monomer concentration) with ADP (at the indicated concentrations) in the absence (△) and presence (■) of Ap_4A (100 μM), observed by isothermal titration calorimetry (ITC) at 20 °C (errors were all ±0.1 kcal/mol of injectant). Buffer conditions were 25 mM Tris-HCl (pH 8.0) with 10 mM KCl and 10 mM $MgCl_2$.

The potential effect of Ap_4A on the ATPase activity of GroEL was investigated using an assay based on a SOURCE Q anion ion exchange column (Amersham Biosciences) mounted on a computer-controlled HPLC system. This allowed repeated samplings of an incubated GroEL/nucleotide mixture at exact time intervals (8 min) and with an identical cycle of washes, loading, and elution for each run. The ion exchange medium chosen gave an excellent separation of nucleotides and polyphosphates (primarily by their phosphate chain length), with a high degree of reproducibility so that peaks could be reliably identified by their retention times after calibration with nucleotide standards. The relative concentrations of nucleotides were then calculated by peak area integration. Initial experiments showed that Ap_4A is stable to incubation with GroEL [37 °C, in 50 mM Tris-HCl (pH 8.0) with 10 mM $MgCl_2$ and 10 mM KCl] for periods of more than 12 h, ruling out any possibility that GroEL has Ap_4Aase activity (data not shown). This result is consistent with the discovery that Ap_4A does not bind in the ATP/ADP binding sites of GroEL since all these sites are dedicated ATPase enzyme active sites. Following this, GroEL ATPase activity was analyzed in the absence of Ap_4A to confirm the utility of the assay system with GroEL (Figure 5a). The rate of disappearance of ATP and other characteristics were as expected from previous reports on the GroEL ATPase (*56*, *57*), with complete hydrolysis of ATP to ADP taking place over the course of ∼40 min at 25 °C, and with ADP being the only significant nucleotide product generated. The effect of 50 μM Ap_4A on GroEL ATPase activity was then investigated at 25, 31, and 37 °C (Figure 5b). Ap_4A appears to induce an only very slight increase in rate at lower temperatures but a more significant (5−10%) enhancement at 37 °C. Enhanced ATPase rates would suggest that the famous "two-stroke motor mechanism" of the GroEL/GroES

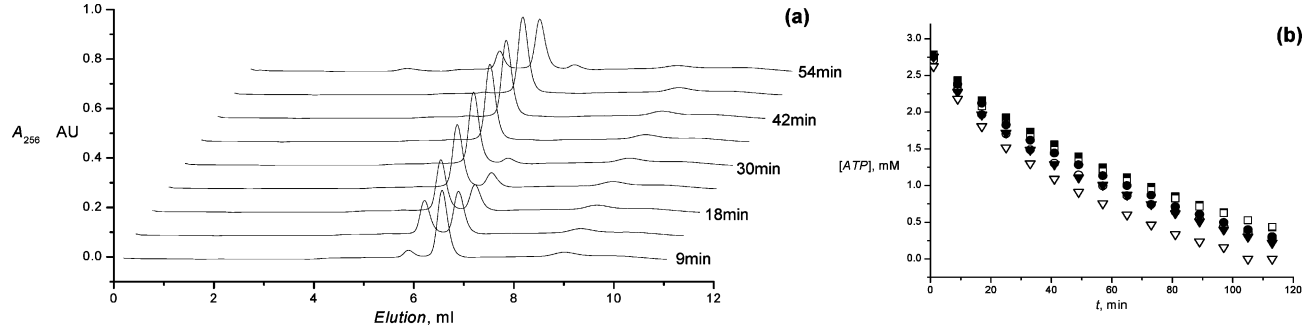

FIGURE 5: Ion exchange HPLC assays of ATP hydrolysis by GroEL (0.5 μM oligomer concentration). (a) Example of raw data traces over a 1 h incubation at 37 °C. These can be integrated to determine the decrease in ATP concentration with time. (b) Illustration of ATPase hydrolysis data for ATP (3 mM) → ADP conversion over time in 10 mM Tris-HCl (pH 8.0) with 10 mM $MgCl_2$ and 10 mM KCl, at different temperatures in the presence and absence of Ap_4A: (■) 25 °C without Ap_4A, (□) 25 °C with 50 μM Ap_4A, (●) 31 °C without Ap_4A, (○) 31 °C with 50 μM Ap_4A, (▼) 37 °C without Ap_4A, and (▽) 37 °C with 50 μM Ap_4A. Error bars (±0.05 mM) were omitted for clarity.

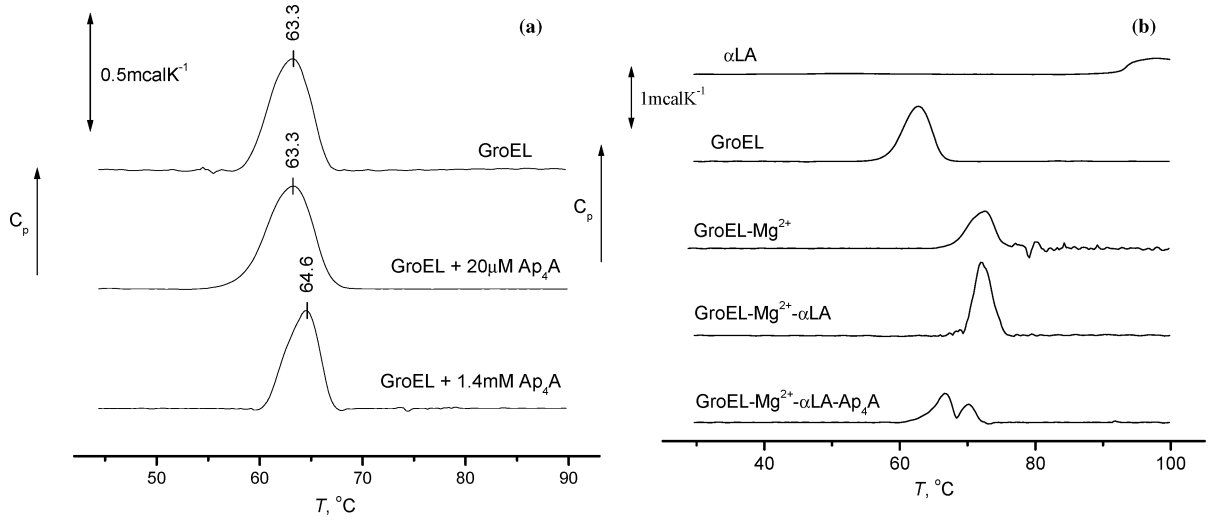

FIGURE 6: Thermal denaturation of GroEL in the presence of various "ligands" observed by differential scanning calorimetry (DSC): (a) GroEL (0.5 μM oligomer concentration, 7 μM monomer concentration) in 25 mM Tris-HCl (pH 8.0) with 1 mM EDTA and with two different concentrations of Ap_4A or (b) α-lactalbumin (αLA) (20 μM) or GroEL (0.5 μM oligomer) in 25 mM Tris-HCl (pH 8.0) (top), GroEL (0.5 μM oligomer) in 25 mM Tris-HCl (pH 8.0) with 1 mM $MgCl_2$ (middle), or the saturated GroEL−αLA complex (0.5 μM GroEL oligomer) in 25 mM Tris-HCl (pH 8.0) with 1 mM $MgCl_2$ without or with Ap_4A (200 μM) (bottom).

molecular chaperone machine may also be accelerated, thereby reducing the routine half-life (6−8 s) for the binding and cavity encapsulation of the unfolded protein substrate by GroEL (*42*, *58*−*61*).

There have been a number of reports about the use of differential scanning calorimetry (DSC) to study the effects of adenine nucleotides on the thermal unfolding of GroEL (*62*, *63*). Therefore, we decided to adopt an equivalent approach to study the effects of Ap_4A. Initial experiments showed that Ap_4A does not affect the melting temperature of GroEL (0.5 μM, homo-oligomer concentration) except at extremely high concentrations (1.4 mM, Figure 6a). Since Mg^{2+} ions (1 mM) are similarly stabilizing, we conclude that the high-concentration Ap_4A stabilization is merely a nonspecific osmolyte effect, and binding of Ap_4A to GroEL does not appear to have any recognizable stabilizing or destabilizing effect on GroEL per se (*63*). However, we observed not only that when GroEL (0.5 μM, homo-oligomer concentration) was combined with an unfolded protein substrate αLA [chosen since this protein may be unfolded in the presence of EDTA and DTT, conditions that do not affect GroEL (*64*)] (20 μM), the saturated GroEL−αLA complex so formed was destabilized in the presence of Ap_4A but also that the melting profile was actually rendered biphasic (Figure 6b). Such a dramatic change suggested that Ap_4A binding was actually promoting differential destabilization of the GroEL−αLA complex and perhaps even thereby encouraging release of αLA. Accordingly, the consequences of binding of Ap_4A to GroEL could be not only to enhance ATPase rates and encourage release of bound ADP (as described above) but also to promote substrate protein release through differential destabilization of the substrate protein−GroEL complex. These features acting in concert might be expected to enhance the chaperoning activities, including the turnover of the GroEL/GroES molecular chaperone machine. But why might such an effect be useful or appropriate?

To try to address this question, we decided to investigate the potential effects of binding of Ap_4A to GroEL on GroEL/GroES-assisted folding and refolding of proteins using our well-established porcine mitochondrial malate dehydrogenase (mMDH) model system (*65*). GroEL/GroES-assisted refolding of mMDH has proven to be a highly informative model system in our hands and in the hands of others trying to understand points of the mechanism of the GroEL/GroES molecular chaperone machine. Following unfolding in 3 M

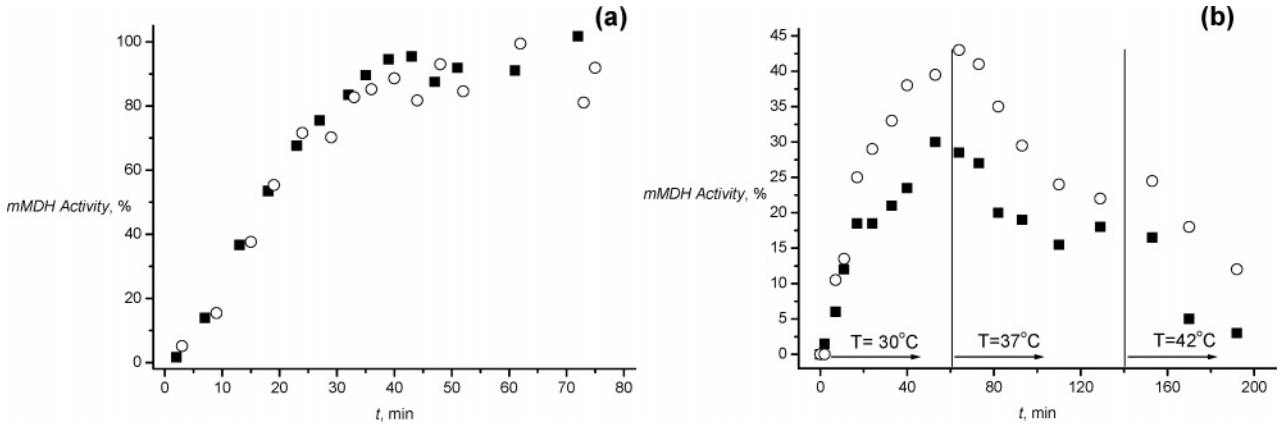

FIGURE 7: GroEL/GroES-assisted refolding of 3 M GuHCl-unfolded mMDH (143 nM) plotted as a percentage of recovered mMDH enzyme activity over time (a) at 20 °C with (■) 2 mM ATP or (○) 2 mM ATP and 0.2 mM Ap_4A or (b) successively at 30, 37, and 42 °C with (■) 0.5 mM ATP or (○) 0.5 mM ATP and 0.2 mM Ap_4A. Errors are ±5% mMDH activity. Other details are in Materials and Methods.

guanidine hydrochloride (GuHCl), mMDH is typically combined with 6- and 12-fold molar excesses of GroEL and GroES, respectively, in the presence of 2 mM ATP, 10 mM Mg^{2+}, and 10 mM K^+ ions. Refolding of mMDH with time is measured as a function of recovery of mMDH enzyme activity with time expressed as a percentage of the enzyme activity of an equivalent quantity of native mMDH kept under the same conditions of buffer, temperature, and concentration.

Studies on GroEL/GroES-assisted and spontaneous mMDH refolding assays were performed in the presence and absence of Ap_4A. The results are shown in Figure 7. Initially, assays performed at 20 °C, a typical assay temperature, revealed that the presence of Ap_4A had no effect on GroEL/GroES-assisted mMDH refolding (Figure 7a). However, at 30 °C, when the yield or efficiency of GroEL/GroES-assisted mMDH refolding typically declines from >90 to ~30% (*64*), the yield of correctly folded mMDH was found to be enhanced by the presence of Ap_4A (Figure 7b). The same effect was found to be true when the assay temperature was further increased stepwise to 37 °C and then to 42 °C (Figure 7b), even as the yield of GroEL/GroES-assisted mMDH refolding declined in the absence of Ap_4A to 20% and then to 3%, respectively. Considering the other biophysical data, we would suggest that enhanced GroEL/GroES chaperoning activities resulting from binding of Ap_4A to GroEL could be a primary reason for the improved yield of refolded mMDH at ≥30 °C. The potential benefits of such behavior will be discussed below.

Studies with CRP. Attempts to investigate binding of Ap_4A to CRP by CD techniques analogous to those used for GroEL gave unsatisfactory results. Despite repeated attempts, we were unable to detect any obvious interactions. A number of extrinsic fluorescence binding titration experiments were performed with *N*-iodoacetyl-*N*′-(5-sulfo-1-naphthyl)ethylenediamine (IAEDANS)-labeled CRP, but although cAMP binding was clearly observed, binding of Ap_4A to CRP was not (results not shown). Therefore, we rapidly concluded that a direct interaction between Ap_4A and CRP is unlikely. Furthermore, we could not detect any interaction between Ap_4A and either the CRP−$cAMP_1$ complex (with two molecules of cAMP bound in the two higher-affinity binding sites) or the CRP−$cAMP_2$ complex (with all four cAMP binding sites saturated).

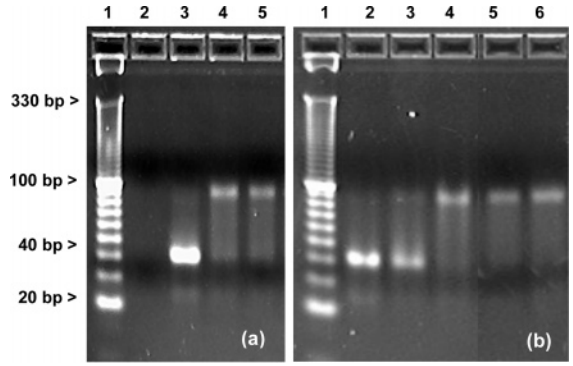

FIGURE 8: E-Gels (4%) depicting CRP−cAMP−consensus DNA complex formation over a range of cAMP and Ap_4A concentrations: (a) lane 1, 10 bp molecular mass markers; lane 2, CRP (2 μM, oligomer concentration); lane 3, DNA (0.38 μM); lane 4, CRP (2 μM), DNA (0.38 μM), and cAMP (5.4 μM); and lane 5, CRP (2 μM), DNA (0.38 μM), and cAMP (100 μM); or (b) lane 1, 10 bp molecular mass markers; lane 2, DNA (0.38 μM) and Ap_4A (182 μM); lane 3, CRP (2 μM), DNA (0.38 μM), and Ap_4A (182 μM); and lanes 4−6, CRP (2 μM), DNA (0.38 μM), Ap_4A (182 μM), and 5.4 μM cAMP (lane 4), 54 μM cAMP (lane 5), or 75 μM cAMP (lane 6).

Accordingly, attention was shifted to CRP−cAMP−DNA complexes beginning with the use of gel retardation assays (*45*, *46*). Such assays are used routinely to study biological macromolecular complex formation with nucleic acids. In our case, aliquots of CRP (each 2 μM, oligomer concentration) were incubated with consensus DNA or control DNA duplexes (40 bp each) in the presence of increasing concentrations of cAMP (from 0 to 100 μM) (Figure 8a). Successful binding of the CRP−$cAMP_1$ complex to the consensus sequence is obvious as DNA mobility was altered from that appropriate for a 40 bp fragment to that of a 90 bp fragment. The critical cAMP concentration at which complete formation of the CRP−$cAMP_1$−DNA ternary complex took place was ~5 μM (Figure 8). As expected, the CRP−$cAMP_1$ complex was unable to bind to the control sequence, and hence, control DNA was not subject to any electrophoretic retardation effects. In this experiment, only interactions between the CRP−$cAMP_1$ complex and DNA were observed. The K_d value of the lower-affinity cAMP binding is several orders of magnitude greater than the K_d value of the higher-affinity cAMP binding sites; therefore, lower-affinity sites will be occupied only in the presence of millimolar cAMP concentrations (*1*, *27*−*29*). Hence, the gel retardation

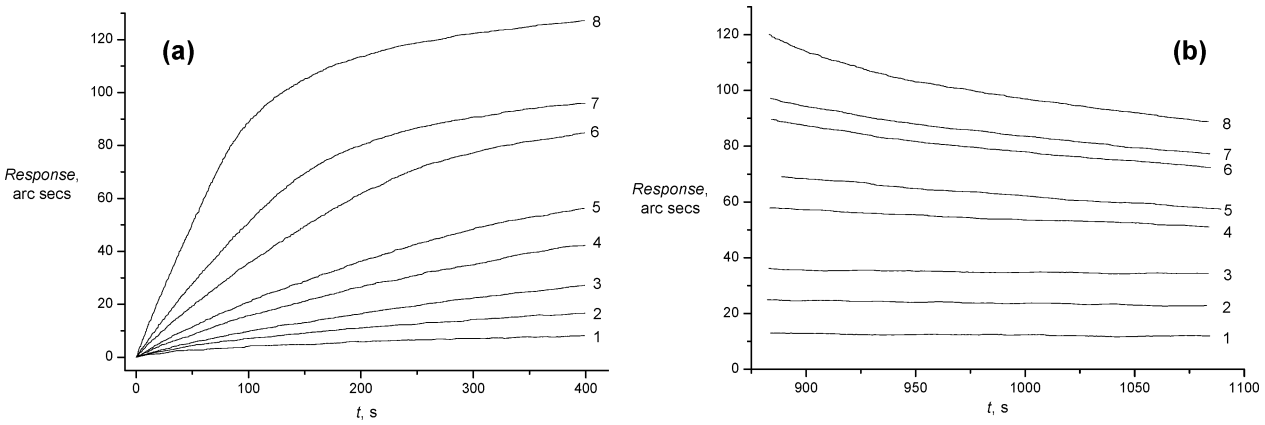

FIGURE 9: IASys instrument responses for the (a) association and (b) dissociation reactions between the CRP−$cAMP_1$ complex and immobilized consensus DNA. cAMP (108 μM) was used with varying CRP concentrations (oligomer concentrations): (1) 1.5, (2) 2.4, (3) 3.6, (4) 4.8, (5) 5.9, (6) 9.5, (7) 15, and (8) 24 nM.

experiments were repeated in the presence of millimolar cAMP concentrations. As expected, consensus DNA was also able to interact with the CRP−$cAMP_2$ complex, causing a retardation effect identical to that observed with the CRP−$cAMP_1$ complex (data not shown), but as before there were no interactions with the control DNA. Having established conditions by which to observe the formation of CRP−$cAMP_1$−DNA and CRP−$cAMP_2$−DNA ternary complexes, we conducted repeat experiments in the presence of Ap_4A. However, we were unable to observe any apparent changes in retardation behavior consistent with perturbed CRP−$cAMP_1$−DNA complex formation in the presence of Ap_4A at concentrations up to 182 μM (Figure 8b). We were equally unable to see any changes under conditions favoring the CRP−$cAMP_2$−DNA complex (results not shown). The clear implication is that Ap_4A has no obvious role to play in regulating CRP−cAMP−DNA complex formation.

Given our inability to detect any Ap_4A effects with standard retardation assay techniques, we decided to employ a resonant mirror biosensor (IAsys) in an attempt to characterize the effects of Ap_4A on the formation of CRP−$cAMP_1$−DNA and CRP−$cAMP_2$−DNA complexes (*67*−*74*). In this instance, the experimental setup required biotin-labeled consensus DNA and control DNA duplexes, preassociated with a streptavidin-loaded biosensor cuvette. Appropriate concentrations of CRP and cAMP were then combined in small volumes (2−10 μL) and introduced to the biosensor chamber (50 μL) so they could interact with immobilized consensus or control DNA duplex. Association and dissociation sensorgram data are shown for the interaction of increasing amounts of the CRP−cAMP1 complex with consensus DNA ([cAMP] = 100 μM) (Figure 9). Sensorgram data for interactions of CRP−$cAMP_1$ and CRP−$cAMP_2$ complexes with consensus DNA were processed, and the binding parameters are given (Table 1). As expected, there were no binding interactions between the CRP−cAMP complex and immobilized control DNA. However, when resonant mirror binding experiments using consensus DNA were repeated in the presence of Ap_4A, there were no significant effects observed on any of the main binding parameters even at >3 mM Ap_4A (data not shown). Therefore, there can be little doubt that CRP, CRP−cAMP complexes, and CRP−cAMP−DNA ternary complexes are not direct targets of Ap_4A action despite the circumstantial evidence in the literature that might suggest otherwise (*22*, *24*, *25*).

Table 1: Kinetic and Thermodynamic Parameters that Describe the Interaction between the CRP−$cAMP_1$ or CRP−$cAMP_2$ Complex and Immobilized Consensus DNA, Measured by IASys[a]

	CRP−$cAMP_1$ complex	CRP−$cAMP_2$ complex
k_{ass} (M^{-1} s^{-1})	$(5.09 \pm 0.54) \times 10^5$	$(9.02 \pm 0.54) \times 10^5$
k_{diss} (s^{-1})	$(4.02 \pm 0.64) \times 10^{-3}$	$(2.46 \pm 0.68) \times 10^{-3}$
K_d (M)	$(9.91 \pm 1.38) \times 10^{-9}$	$(2.73 \pm 0.77) \times 10^{-9}$
$K_{d,response}$[b] (M)	$(6.18 \pm 2.19) \times 10^{-9}$	$(3.85 \pm 0.82) \times 10^{-9}$

[a] Dissociation constant K_d is evaluated from k_{ass} and k_{diss}. [b] Dissociation constant $K_{d,response}$ is calculated from equilibrium response measurements.

DISCUSSION

In the case of GroEL, the data appear to interlock to support the view that binding of Ap_4A to GroEL enhances ATPase rates at higher temperatures, encourages the release of bound ADP, and may promote substrate protein release through differential destabilization of the substrate protein−GroEL complex. We suggest that such effects brought about by binding of Ap_4A to GroEL should result in enhanced GroEL/GroES chaperoning activities that could be a primary reason for the improved yields of refolded substrate protein resulting from GroEL/GroES-assisted folding and refolding of the unfolded substrate protein at ≥30 °C, in the presence of Ap_4A. This effect of Ap_4A on GroEL makes an interesting juxtaposition with respect to the known behavior of GroEL at higher temperatures. While GroEL is certainly a molecular chaperone, at higher temperatures (especially >37 °C), the chaperone activity is known to be decreased in favor of a protein depot or storage function, presumably allowing for the binding of stress-unfolded proteins to protect exposed hydrophobic surfaces and thereby preventing protein aggregation that is otherwise toxic to cells. Higher temperatures induce conformational changes in GroEL that stabilize the structure and enhance the storage function. These changes are typically reversed at lower temperatures whereupon chaperoning activities are increasingly restored (*66*, *75*, *76*). Arguably, the consequences of binding of Ap_4A to GroEL are to promote the chaperoning activities of GroEL over depot/storage activities, and hence, Ap_4A appears to act in ways consistent with opposition to the effects of higher

temperatures on GroEL. Such a suggestion would certainly be consistent, in particular, with the biphasic destabilization of the saturated GroEL−αLA complex observed by DSC (Figure 6) and the ability of Ap_4A to enhance the yield of active refolded mMDH from GroEL/GroES-assisted refolding of unfolded mMDH at >30 °C (Figure 7).

But then why should Ap_4A have the potential capacity to oppose the protein depot or storage function of GroEL in favor of chaperoning activities? The answer may rest with the realization that Ap_4A is not a stress "alarmone" as originally thought but may be a modulator of stress responses that could function to help cells sustain some kind of basic physiology during stress and then immediately poststress, aid cellular recovery, and assist in the return to normal cellular physiology and metabolism (*77*−*80*). Arguably, the binding of Ap_4A to GroEL could be considered to have some kind of modulator or "repressor" function, reducing the likelihood that GroEL converts to the depot/storage conformation from an active molecular chaperone conformational state. In so doing, Ap_4A could contribute significantly to *E. coli*'s ability to sustain a "skeleton" physiology and metabolism during stress and then, immediately poststress, aid in the restoration of normal physiology and metabolism.

The binding of Ap_4A to GroEL is also interesting in a number of ways. This is the first time, to the best of our knowledge, that an allosteric modulator of GroEL function has been identified that not only exercises some apparent conformational control over GroEL but also enhances ATPase rates at higher temperatures (Figure 5) and reduces the binding affinity of ADP (Figure 4). Ap_4A binds to GroEL at a site completely different from the ATP/ADP−ATPase binding site located in each GroEL monomer, as demonstrated by CD titration binding experiments (Figure 2), affinity probe binding experiments (Figure 3), and ITC studies (Figure 4). The ITC studies in particular indicate that Ap_4A and ADP bind to GroEL by substantially different mechanisms consistent with binding to substantially different binding pockets. We do not yet know where this new binding site must be in each monomer, but it is tempting to speculate that each Ap_4A binding site in each GroEL monomer might be closely associated with the lateral holes located between the equatorial and apical domains of each GroEL 7mer ring in two parallel rows on the sides of each GroEL 14mer. However, tempting though such speculation might be, it still remains to be proved!

The data presented in this paper represent a story of mixed fortunes. In the case of studies with CRP, Ap_4A does not appear to have any obvious direct role with CRP that we are able to discern, so we are forced to look elsewhere for an explanation as to how Ap_4A renders bacteria nonmotile and unable to biosynthesize the enzymes required for lactose and galactose metabolism (*22*). The CRP−$cAMP_1$ complex is a positive regulator of operon transcription at more than 100 promoter sites, but one whose function can be offset by repressors such as the *lac* repressor of the *lac* operon. In this case, binding of the *lac* repressor in the *lac* promoter has to be suppressed for the positive regulator to function. In our work, we appear to have demonstrated that Ap_4A does not act as a modulator of CRP activity at the level of CRP alone or even at the level of the formation of the CRP−$cAMP_1$ complex. In addition, we cannot see any sign of interference at the level of CRP−$cAMP_1$−DNA complex formation. However, this does not rule out the possibility that Ap_4A could function as a modulator or repressor of operons involving CRP either by direct binding to promoter DNA or by binding to and activating *lac* repressor-like proteins that are able to prevent the CRP−$cAMP_1$ positive regulator from operating.

There is also a clear possibility that we may have identified the wrong Ap_4A target by forming a hypothesis based upon literature phenotypes. Therefore, there must now be a real case for revisiting the original pioneering work of Johnstone and Farr (*9*), and we must seek to use molecules such as dial-mant-Ap_4A to provide a more in-depth affinity column/proteomics-based approach for the identification of new and alternative Ap_4A binding proteins in *E. coli*, in other prokaryotes, and even in eukaryotic cells (*44*). If Ap_4A is indeed a modulator of stress responses with repressor-like functions, then there are certain to be many more molecular partners for Ap_4A and other Ap_nA's yet to be uncovered. If these can be identified and studied, then this is sure to usher in an important new era of discovery in dinucleoside polyphosphate research.

ACKNOWLEDGMENT

We thank Prof. H. Aiba of the Department of Molecular Biology at Nagoya University (Nagoya, Japan) for the kind gift of *E. coli* strain PP47, carrying plasmid pHA7.

REFERENCES

1. Garrison, P. N., and Barnes, L. D. (1992) in *Ap_4A and Other Dinucleoside Polyphosphates* (McLennan, A. G., Ed.) pp 29−61, CRC Press, Boca Raton, FL.
2. McLennan, A. G. (2000) Dinucleoside polyphosphates: Friend or foe? *Pharmacol. Ther. 87*, 73−89.
3. McLennan, A. G., Barnes, L. D., Blackburn, G. M., Brenner, C., Guranowski, A., Miller, A. D., Rovira, J. M., Rotlan, P., Soria, B., Tanner, J. A., and Sillero, A. (2001) Recent progress in the study of the intracellular functions of diadenosine polyphosphates, *Drug Dev. Res. 52*, 249−259.
4. Vartanian, A., Alexandrov, I., Prudowski, I., McLennan, A., and Kisselev, L. (1999) Ap4A induces apoptosis in human cultured cells, *FEBS Lett. 456*, 175−180.
5. Luthje, J., Baringer, J., and Ogilvie, A. (1985) Effects of diadenosine triphosphate (Ap3A) and diadenosine tetraphosphate (Ap4A) on platelet aggregation in unfractionated human blood, *Blut 51*, 405−413.
6. Pintor, J., Peral, A., Pelaez, T., Martin, S., and Hoyle, C. H. (2003) Presence of diadenosine polyphosphates in the aqueous humor: Their effect on intraocular pressure, *J. Pharmacol. Exp. Ther. 304*, 342−348.
7. Lee, P. C., Bochner, B. R., and Ames, B. N. (1983) AppppA, heat-shock stress, and cell oxidation, *Proc. Natl. Acad. Sci. U.S.A. 80*, 7496−7500.
8. Bochner, B. R., Lee, P. C., Wilson, S. W., Cutler, C. W., and Ames, B. N. (1984) AppppA and related adenylylated nucleotides are synthesized as a consequence of oxidation stress, *Cell 37*, 225−232.
9. Johnstone, D. B., and Farr, S. B. (1991) AppppA binds to several proteins in *Escherichia coli*, including the heat shock and oxidative stress proteins DnaK, GroEL, E89, C45 and C40, *EMBO J. 10*, 3897−3904.
10. Braig, K., Simon, M., Furuya, F., Hainfeld, J. F., and Horwich, A. L. (1993) A polypeptide bound by the chaperonin groEL is localized within a central cavity, *Proc. Natl. Acad. Sci. U.S.A. 90*, 3978−3982.
11. Braig, K., Adams, P. D., and Brunger, A. T. (1995) Conformational variability in the refined structure of the chaperonin GroEL at 2.8 Å resolution, *Nat. Struct. Biol. 2*, 1083−1094.
12. Valle, F., Derose, J. A., Dietler, G., Kawe, M., Pluckthun, A., and Semenza, G. (2001) Imaging the native structure of the

chaperone protein GroEL without fixation using atomic force microscopy, *J. Microsc. 203*, 195−198.
13. Horst, R., Bertelsen, E. B., Fiaux, J., Wider, G., Horwich, A. L., and Wuthrich, K. (2005) Direct NMR observation of a substrate protein bound to the chaperonin GroEL, *Proc. Natl. Acad. Sci. U.S.A. 102*, 12748−12753.
14. Bukau, B., and Horwich, A. L. (1998) The Hsp70 and Hsp60 chaperone machines, *Cell 92*, 351−366.
15. Gottesman, M. E., and Hendrickson, W. A. (2000) Protein folding and unfolding by *Escherichia coli* chaperones and chaperonins, *Curr. Opin. Microbiol. 3*, 197−202.
16. Gutsche, I., Essen, L. O., and Baumeister, W. (1999) Group II chaperonins: New TRiC(k)s and turns of a protein folding machine, *J. Mol. Biol. 293*, 295−312.
17. Hartle, J. E., II, Prpic, V., Siddhanti, S. R., Spurney, R. F., and Quarles, L. D. (1996) Differential regulation of receptor-stimulated cyclic adenosine monophosphate production by polyvalent cations in MC3T3-E1 osteoblasts, *J. Bone Miner. Res. 11*, 789−799.
18. Saibil, H. (2000) Molecular chaperones: Containers and surfaces for folding, stabilising or unfolding proteins, *Curr. Opin. Struct. Biol. 10*, 251−258.
19. Teter, S. A., Houry, W. A., Ang, D., Tradler, T., Rockabrand, D., Fischer, G., Blum, P., Georgopoulos, C., and Hartl, F. U. (1999) Polypeptide flux through bacterial Hsp70: DnaK cooperates with trigger factor in chaperoning nascent chains, *Cell 97*, 755−765.
20. Frydman, J. (2001) Folding of newly translated proteins in vivo: The role of molecular chaperones, *Annu. Rev. Biochem. 70*, 603−647.
21. Erbse, A., Dougan, D. A., and Bukau, B. (2003) A folding machine for many but a master of none, *Nat. Struct. Biol. 10*, 84−86.
22. Farr, S. B., Arnosti, D. N., Chamberlin, M. J., and Ames, B. N. (1989) An apaH mutation causes AppppA to accumulate and affects motility and catabolite repression in *Escherichia coli*, *Proc. Natl. Acad. Sci. U.S.A. 86*, 5010−5014.
23. Passner, J. M., Schultz, S. C., and Steitz, T. A. (2000) Modeling the cAMP-induced allosteric transition using the crystal structure of CAP-cAMP at 2.1 Å resolution, *J. Mol. Biol. 304*, 847−859.
24. Plateau, P., and Blanquet, S. (1994) Dinucleoside oligophosphates in micro-organisms, *Adv. Microb. Physiol. 36*, 81−109.
25. Kitzler, J. W., Farr, S. B., and Ames, B. N. (1992) in *Ap_4A and Other Dinucleoside Polyphosphates* (McLennan, A. G., Ed.) pp 135−149, CRC Press, Boca Raton, FL.
26. Budavari, S. (1996) *Merck Index*, 12th ed., Merck & Co. Inc., Rahway, NJ.
27. Epstein, W., Rothman-Denes, L. B., and Hesse, J. (1975) Adenosine 3′:5′-cyclic monophosphate as mediator of catabolite repression in *Escherichia coli*, *Proc. Natl. Acad. Sci. U.S.A. 72*, 2300−2304.
28. Takahashi, M., Blazy, B., and Baudras, A. (1980) An equilibrium study of the cooperative binding of adenosine cyclic 3′,5′-monophosphate and guanosine cyclic 3′,5′-monophosphate to the adenosine cyclic 3′,5′-monophosphate receptor protein from *Escherichia coli*, *Biochemistry 19*, 5124−5130.
29. Sambrook, J., and Russell, D. W. (2001) *Molecular Cloning. A Laboratory Manual*, 3rd ed., p 6.11, Cold Spring Harbor Laboratory Press, Plainview, NY.
30. Ryu, S., Kim, J., Adhya, S., and Garges, S. (1993) Pivotal role of amino acid at position 138 in the allosteric hinge reorientation of cAMP receptor protein, *Proc. Natl. Acad. Sci. U.S.A. 90*, 75−79.
31. Wu, F. Y., Nath, K., and Wu, C. W. (1974) Conformational transitions of cyclic adenosine monophosphate receptor protein of *Escherichia coli*. A fluorescent probe study, *Biochemistry 13*, 2567−2572.
32. Creighton, T. E. (1993) *Proteins: Structures and Molecular Properties*, 2nd ed., W. H. Freeman and Company, New York.
33. Harman, J. G. (2001) Allosteric regulation of the cAMP receptor protein, *Biochim. Biophys. Acta 1547*, 1−17.
34. Bruckner, R., and Titgemeyer, F. (2002) Carbon catabolite repression in bacteria: Choice of the carbon source and autoregulatory limitation of sugar utilization, *FEMS Microbiol. Lett. 209*, 141−148.
35. Busby, S., and Ebright, R. H. (1999) Transcription activation by catabolite activator protein (CAP), *J. Mol. Biol. 293*, 199−213.
36. Colland, F., Barth, M., Hengge-Aronis, R., and Kolb, A. (2000) σ factor selectivity of *Escherichia coli* RNA polymerase: Role for CRP, IHF and lrp transcription factors, *EMBO J. 19*, 3028−3037.
37. Holler, E., Holmquist, B., Vallee, B. L., Taneja, K., and Zamecnik, P. (1983) Circular dichroism and ordered structure of bisnucleoside oligophosphates and their Zn^{2+} and Mg^{2+} complexes, *Biochemistry 22*, 4924−4933.
38. Gill, S. C., and von Hippel, P. H. (1989) Calculation of protein extinction coefficients from amino acid sequence data, *Anal. Biochem. 182*, 319−326.
39. Kohler, R. J., Preuss, M., and Miller, A. D. (2000) Design of a molecular chaperone-assisted protein folding bioreactor, *Biotechnol. Prog. 16*, 671−675.
40. Hutchinson, J. P., el-Thaher, T. S., and Miller, A. D. (1994) Refolding and recognition of mitochondrial malate dehydrogenase by *Escherichia coli* chaperonins cpn 60 (groEL) and cpn10 (groES), *Biochem. J. 302* (Part 2), 405−410.
41. Tabona, P., Reddi, K., Khan, S., Nair, S. P., Crean, S. J., Meghji, S., Wilson, M., Preuss, M., Miller, A. D., Poole, S., Carne, S., and Henderson, B. (1998) Homogeneous *Escherichia coli* chaperonin 60 induces IL-1β and IL-6 gene expression in human monocytes by a mechanism independent of protein conformation, *J. Immunol. 161*, 1414−1421.
42. Preuss, M., Hutchinson, J. P., and Miller, A. D. (1999) Secondary structure forming propensity coupled with amphiphilicity is an optimal motif in a peptide or protein for association with chaperonin 60 (GroEL), *Biochemistry 38*, 10272−10286.
43. Wright, M., and Miller, A. D. (2004) Synthesis of novel fluorescent-labelled dinucleoside polyphosphates, *Bioorg. Med. Chem. Lett. 14*, 2813−2816.
44. Wright, M., and Miller, A. D. (2006) Novel fluorescent labelled affinity probes for diadenosine-5′,5‴-P1,P4-tetraphosphate (Ap4A)-binding studies, *Bioorg. Med. Chem. Lett. 16*, 943−948.
45. Aoki, K., Taguchi, H., Shindo, Y., Yoshida, M., Ogasahara, K., Yutani, K., and Tanaka, N. (1997) Calorimetric observation of a GroEL-protein binding reaction with little contribution of hydrophobic interaction, *J. Biol. Chem. 272*, 32158−32162.
46. Garner, M. M., and Revzin, A. (1981) A gel electrophoresis method for quantifying the binding of proteins to specific DNA regions: Application to components of the *Escherichia coli* lactose operon regulatory system, *Nucleic Acids Res. 9*, 3047−3060.
47. Fried, M., and Crothers, D. M. (1981) Equilibria and kinetics of lac repressor-operator interactions by polyacrylamide gel electrophoresis, *Nucleic Acids Res. 9*, 6505−6525.
48. Affinity Sensors (1997) *IAsys plus Methods Guide*, Human-Computer Interfaces Ltd., Cambridge, U.K.
49. George, A. J., French, R. R., and Glennie, M. J. (1995) Measurement of kinetic binding constants of a panel of anti-saporin antibodies using a resonant mirror biosensor, *J. Immunol. Methods 183*, 51−63.
50. Holler, E. (1984) Noncovalent complexes of diadenosine 5′,5‴-P1,P4-tetraphosphate with divalent metal ions, biogenic amines, proteins and poly(dT), *Biochem. Biophys. Res. Commun. 120*, 1037−1043.
51. Klotz, I. M., and Hunston, D. L. (1971) Properties of graphical representations of multiple classes of binding sites, *Biochemistry 10*, 3065−3069.
52. Tanner, J. A., Abowath, A., and Miller, A. D. (2002) Isothermal titration calorimetry reveals a zinc ion as an atomic switch in the diadenosine polyphosphates, *J. Biol. Chem. 277* (5), 3073−3078.
53. Hiratsuka, T. (1983) New ribose-modified fluorescent analogs of adenine and guanine nucleotides available as substrates for various enzymes, *Biochim. Biophys. Acta 742*, 496−508.
54. Thomson, G. J., Coggins, J. R., and Price, N. C. (1993) Studies of the ATP binding site in the chaperone protein GroEL (cpn60), *Biochem. Soc. Trans. 21*, 61S.
55. Terada, T. P., and Kuwajima, K. (1999) Thermodynamics of nucleotide binding to the chaperonin GroEL studied by isothermal titration calorimetry: Evidence for noncooperative nucleotide binding, *Biochim. Biophys. Acta 1431*, 269−281.
56. Jackson, G. S., Staniforth, R. A., Halsall, D. J., Atkinson, T., Holbrook, J. J., Clarke, A. R., and Burston, S. G. (1993) Binding and hydrolysis of nucleotides in the chaperonin catalytic cycle: Implications for the mechanism of assisted protein folding, *Biochemistry 32*, 2554−2563.
57. Todd, M. J., Viitanen, P. V., and Lorimer, G. H. (1993) Hydrolysis of adenosine 5′-triphosphate by *Escherichia coli* GroEL: Effects of GroES and potassium ion, *Biochemistry 32*, 8560−8567.
58. Preuss, M., and Miller, A. D. (2000) The affinity of the GroEL/GroES complex for peptides under conditions of protein folding, *FEBS Lett. 466*, 75−79.
59. Xu, Z., and Sigler, P. B. (1998) GroEL/GroES: Structure and function of a two-stroke folding machine, *J. Struct. Biol. 124*, 129−141.

60. Kad, N. M., Ranson, N. A., Cliff, M. J., and Clarke, A. R. (1998) Asymmetry, commitment and inhibition in the GroE ATPase cycle impose alternating functions on the two GroEL rings, *J. Mol. Biol. 278*, 267−278.
61. Lorimer, G. (1997) Protein folding. Folding with a two-stroke motor, *Nature 388*, 720−721, 723.
62. Galan, A., Llorca, O., Valpuesta, J. M., Perez-Perez, J., Carrascosa, J. L., Menendez, M., Banuelos, S., and Muga, A. (1999) ATP hydrolysis induces an intermediate conformational state in GroEL, *Eur. J. Biochem. 259*, 347−355.
63. Surin, A. K., Kotova, N. V., Kashparov, I. A., Marchenkov, V. V., Marchenkova, S., and Semisotnov, G. V. (1997) Ligands regulate GroEL thermostability, *FEBS Lett. 405*, 260−262.
64. Hayer-Hartl, M. K., Ewbank, J. J., Creighton, T. E., and Hartl, F. U. (1994) Conformational specificity of the chaperonin GroEL for the compact folding intermediates of alpha-lactalbumin, *EMBO J. 13*, 3192−3202.
65. Miller, A. D., Maghlaoui, K., Albanese, G., Kleinjan, D. A., and Smith, C. (1993) *Escherichia coli* chaperonins cpn60 (groEL) and cpn10 (groES) do not catalyse the refolding of mitochondrial malate dehydrogenase, *Biochem. J. 291*, 139−144.
66. Llorca, O., Galan, A., Carrascosa, J. L., Muga, A., and Valpuesta, J. M. (1998) GroEL under heat-shock. Switching from a folding to a storing function, *J. Biol. Chem. 273*, 32587−32594.
67. Ebright, R. H., Ebright, Y. W., and Gunasekera, A. (1989) Consensus DNA site for the *Escherichia coli* catabolite gene activator protein (CAP): CAP exhibits a 450-fold higher affinity for the consensus DNA site than for the *E. coli* lac DNA site, *Nucleic Acids Res. 17*, 10295−10305.
68. Shi, Y., Wang, S., Krueger, S., and Schwarz, F. P. (1999) Effect of mutations at the monomer-monomer interface of cAMP receptor protein on specific DNA binding, *J. Biol. Chem. 274*, 6946−6956.
69. Gunasekera, A., Ebright, Y. W., and Ebright, R. H. (1992) DNA sequence determinants for binding of the *Escherichia coli* catabolite gene activator protein, *J. Biol. Chem. 267*, 14713−14720.
70. Leu, S. F., Baker, C. H., Lee, E. J., and Harman, J. G. (1999) Position 127 amino acid substitutions affect the formation of CRP:cAMP:lacP complexes but not CRP:cAMP:RNA polymerase complexes at lacP, *Biochemistry 38*, 6222−6230.
71. Heyduk, T., and Lee, J. C. (1990) Application of fluorescence energy transfer and polarization to monitor *Escherichia coli* cAMP receptor protein and lac promoter interaction, *Proc. Natl. Acad. Sci. U.S.A. 87*, 1744−1748.
72. Liu-Johnson, H. N., Gartenberg, M. R., and Crothers, D. M. (1986) The DNA binding domain and bending angle of *E. coli* CAP protein, *Cell 47*, 995−1005.
73. Fried, M. G., and Crothers, D. M. (1984) Kinetics and mechanism in the reaction of gene regulatory proteins with DNA, *J. Mol. Biol. 172*, 263−282.
74. Vossen, K. M., Wolz, R., Daugherty, M. A., and Fried, M. G. (1997) Role of macromolecular hydration in the binding of the *Escherichia coli* cyclic AMP receptor to DNA, *Biochemistry 36*, 11640−11647.
75. Cabiscol, E., Belli, G., Tamarit, J., Echave, P., Herrero, E., and Ros, J. (2002) Mitochondrial Hsp60, resistance to oxidative stress, and the labile iron pool are closely connected in *Saccharomyces cerevisiae*, *J. Biol. Chem. 277*, 44531−44538.
76. Melkani, G. C., Zardeneta, G., and Mendoza, J. A. (2005) On the chaperonin activity of GroEL at heat-shock temperature, *Int. J. Biochem. Cell Biol. 37*, 1375−1385.
77. Palfi, Z., Suranyi, G., and Borbely, G. (1991) Alterations in the accumulation of adenylylated nucleotides in heavy-metal-ion-stressed and heat-stressed *Synechococcus* sp. strain PCC 6301, a cyanobacterium, in light and dark, *Biochem. J. 276* (Part 2), 487−491.
78. Brevet, A., Chen, J., Leveque, F., Plateau, P., and Blanquet, S. (1989) In vivo synthesis of adenylylated bis(5′-nucleosidyl) tetraphosphates (Ap4N) by *Escherichia coli* aminoacyl-tRNA synthetases, *Proc. Natl. Acad. Sci. U.S.A. 86*, 8275−8279.
79. Guedon, G. F., Gilson, G. J., Ebel, J. P., Befort, N. M., and Remy, P. M. (1986) Lack of correlation between extensive accumulation of bisnucleoside polyphosphates and the heat-shock response in eukaryotic cells, *J. Biol. Chem. 261*, 16459−16465.
80. Segal, E., and Le Pecq, J. B. (1986) Relationship between cellular diadenosine 5′,5‴-P1,P4-tetraphosphate level, cell density, cell growth stimulation and toxic stresses, *Exp. Cell Res. 167*, 119−126.

BI052529K